Gravity-Induced Errors in Airborne Inertial Navigation

David W. Harriman* and J. Chris Harrison†
Geodynamics Corporation, Santa Barbara, California

This paper describes a simple yet powerful statistical technique for calculating the effects of errors in a detailed navigation gravity model on an inertial navigation system (INS) traveling a great circle flight path. Error variances in the horizontal position and velocity of an aircraft are computed from the time-dependent frequency response of the inertial navigation system and the power spectral densities of errors in the along- and cross-track gravity disturbance components derived from the navigation gravity model. The power spectra are obtained by first computing the spectrum of the vertical gravity disturbance errors using available degree spectrum models and results of mean gravity value estimation error analyses, then using fundamental equations of gravitational potential theory to relate this vertical disturbance error spectrum to the desired along- and cross-track disturbance error spectra. These spectra have dramatically different shapes with the cross-track component having much greater power at low frequencies. Since the response of a lightly damped INS is sharply peaked at low frequencies, nearly all of the navigation error is initially induced in the cross-track direction and accumulates in the along-track direction primarily through Coriolis coupling.

I. Introduction

WITH the development of increasingly accurate inertial navigation system (INS) hardware, the need has arisen for correspondingly accurate navigation gravity models (NGMs). An NGM based on the available data, including surface gravimetry and satellite altimetry, can provide a detailed description of intermediate and long wavelength variations of gravity disturbances. A statistical error analysis of an INS employing such an NGM requires error models more vesatile than the attenuated white noise models[1] or the two-parameter Markov models[2,3] commonly used to represent the errors in a simple ellipsoidal NGM. This paper describes such a statistical error analysis method, which computes the INS errors due to both the short wavelengths omitted from the NGM and the errors in the estimation of those longer wavelengths included in the NGM.

This analysis addresses an aircraft traveling at constant speed along a great circle path and employing an INS whose sole source of error is the NGM used to compute the horizontal components of the gravity disturbance vector at the aircraft position (the vertical position of the aircraft is assumed to be accurately determined by noninertial instrumentation, e.g., radar or barometric altimeters). The standard deviations of the errors in the indicated position and velocity of the aircraft are calculated as functions of the flight time, flight altitude and speed, velocity error damping factor of the INS, and spatial resolution and accuracy of the NGM.

Errors in the horizontal components of the gravity disturbance vector are propagated into aircraft position and velocity errors by means of the INS frequency-response function. This error analysis is similar to that reported by Bernstein and Hess,[4] but incorporates the following significant improvements: 1) time-dependent response functions are used, permitting evaluation of transient as well as steady-state response and thus the response of an undamped INS; 2) important effects due to Earth rotation, which were incorrectly assessed as negligible in Ref. 4, have been included; 3) the frequency-domain upward continuation of gravity disturbance to aircraft altitude is treated more rigorously, leading to conclusions significantly different from those in Ref. 4; 4) a coordinate system oriented along- and cross-track is used, leading to the realization that INS error variances in these two directions can differ by more than an order of magnitude; and 5) the horizontal gravity disturbance error spectra are derived by a more rigorous method which does not require these spectra to fit a simple two-parameter model. The solution of the time-dependent, Coriolis-coupled INS error equation and the derivation of the dramatic differences between along- and cross-track gravity disturbance error specta at low frequencies are considered the primary contributions of this paper. Although coordinate systems oriented along- and cross-track have been used in statistical geodesy and INS error analysis for many years and differences between the along- and cross-track gravity disturbances are well known,[2,3] it has not been generally recognized that these differences are greatly amplified when the comparison is made between along- and cross-track gravity disturbance errors after compensation by a detailed NGM.

INS error analyses commonly employ linear state-space methods or detailed flight simulation techniques. In comparison to the frequency-domain approach, the linear state-space methods have the advantage of accommodating the effects of a wide variety of external aids but impose the undesirable restriction that errors must be described by Markov models. Averaging the results from a large number of deterministic simulations (i.e., the Monte Carlo method) has the advantage that complicated flight paths, nonstationary gravity error models, and the effects of external aids can be treated, but the necessity of computing an ensemble of cases for each set of parameter values for which results are desired makes such analyses extremely expensive and time-consuming.[5] In contrast, the frequency-domain analysis presented herein allows one to quickly determine the dependence of the INS errors on each important parameter and, in addition, yields considerable insight into the mechanisms by which NGM errors are propagated through the INS.

II. Fundamental Equations

A right-handed Cartesian coordinate system is used with the z axis directed upward along the local geodetic vertical; the x

Presented as Paper 84-1873 at the AIAA Guidance and Control Conference, Seattle, WA, Aug. 20-22, 1984; received July 19, 1985; revision received Dec. 6, 1985.

*Member Professional Staff, Systems Engineering Department.
†Senior Staff Member, Santa Barbara Operations.

axis is horizontal and in the plane of the great circle path (along-track), while the y axis is horizontal and perpendicular to this plane (cross-track). The INS position errors δx and δy are related to the gravity disturbance errors δg_x and δg_y by the following equations:

$$\delta\ddot{x} + 2\zeta\omega_s\delta\dot{x} + \omega_s^2\delta x - 2\Omega_e\sin\phi\delta\dot{y} = \delta g_x \tag{1}$$

and

$$\delta\ddot{y} + 2\zeta\omega_s\delta\dot{y} + \omega_s^2\delta y + 2\Omega_e\sin\phi\delta\dot{x} = \delta g_y \tag{2}$$

where $\omega_s = \sqrt{g/R}$ is the Schuler frequency, ζ the velocity error damping factor, Ω_e the Earth's rotational rate, and ϕ the aircraft geodetic latitude. A derivation of these equations is given in the Appendix of Ref. 6.

There are two advantages in using a coordinate system in which the horizontal axes are oriented along- and cross-track rather than north and east. First, in the latter system, the Coriolis coupling terms are significantly more complicated (additional terms appear which are proportional to the time derivative of the longitude). Second, and more important, the statistical representations of the gravity disturbance errors are simplified because the global average of the cross correlation between along- and cross-track gravity disturbance is zero.[7]

The first step in solving Eqs. (1) and (2) for the position and velocity errors is to derive the frequency-response functions (or system transfer functions), which are defined as follows: the direct frequency-response function $G^2(\omega,t)$ is the mean square error along an axis which results from a 1 mgal (0.001 cm/s^2) periodic input of frequency ω along that axis, and the transverse frequency-response function $g^2(\omega,t)$ is the mean square error along an axis which results from a 1 mgal periodic input of frequency ω along the perpendicular axis. Both have units of ft^2/mgal^2 and depend on frequency, time, damping factor, and latitude. The transverse response function is a result of Earth's rotation, which couples the errors in the x and y directions.

The next step is to derive the power spectral densities (psds) of the along- and cross-track gravity disturbance errors δg_x and δg_y. Two types of errors are considered: first, those errors due to short wavelength variations in the gravity potential which are not modeled (omission errors), and, second, errors due to incorrectly modeling the longer wavelength variations (commission errors). The psds of along- and cross-track disturbance errors [denoted $S_x(\omega,z)$ and $S_y(\omega,z)$, respectively] which result from each of the NGM errors are calculated in Sec. IV.

Finally, the variances of along- and cross-track position errors are given by

$$\sigma_x^2(t,z) = \int_0^\infty G^2(\omega,t)S_x(\omega,z)\mathrm{d}\omega + \int_0^\infty g^2(\omega,t)S_y(\omega,z)\mathrm{d}\omega \tag{3}$$

and

$$\sigma_y^2(t,z) = \int_0^\infty G^2(\omega,t)S_y(\omega,z)\mathrm{d}\omega + \int_0^\infty g^2(m,t)S_x(\omega,z)\mathrm{d}\omega \tag{4}$$

By differentiating Eqs. (1) and (2) it can be shown that the velocity error variances $\sigma_{vx}^2(t,z)$ and $\sigma_{vy}^2(t,z)$ satisfy similar equations except that the response functions are multiplied by the square of the frequency, i.e.,

$$\sigma_{vx}^2(t,z) = \int_0^\infty G^2(\omega,t)S_x(\omega,z)\omega^2\mathrm{d}\omega + \int_0^\infty g^2(\omega,t)S_y(\omega,z)\omega^2\mathrm{d}\omega \tag{5}$$

and

$$\sigma_{vy}^2(t,z) = \int_0^\infty G^2(\omega,t)S_y(\omega,z)\omega^2\mathrm{d}\omega + \int_0^\infty g^2(\omega,t)S_x(\omega,z)\omega^2\mathrm{d}\omega \tag{6}$$

III. INS Frequency Response

If the inputs in Eqs. (1) and (2) are

$$\delta g_x = \cos(\omega t + \alpha) \text{ and } \delta g_y = 0 \tag{7}$$

then, by the definitions of the frequency-response functions given in Sec. II, it follows that

$$G^2(\omega,t) = \overline{\delta x^2} \text{ and } g^2(\omega,t) = \overline{\delta y^2} \tag{8}$$

where the overbar denotes a uniformly weighted average over the phase α of the gravity error inputs. Thus, the response functions are found by solving the equations

$$\delta\ddot{x} + 2\zeta\omega_s\delta\dot{x} + \omega_s^2\delta x - 2\Omega_e\sin\phi\delta\dot{y} = \cos(\omega t + \alpha) \tag{9}$$

and

$$\delta\ddot{y} + 2\zeta\omega_s\delta\dot{y} + \omega_s^2\delta y + 2\Omega_e\sin\phi\delta\dot{x} = 0 \tag{10}$$

for the quantities $\overline{\delta x^2}$ and $\overline{\delta y^2}$.

As the latitude of the aircraft varies, the Coriolis coupling term changes with time, greatly complicating these equations. This difficulty is overcome by replacing the factor $\sin\phi$ with its average value $\langle\sin\phi\rangle$ over the flight path. This is a good approximation except for north-south flight paths at low latitudes.

Equations (9) and (10) are solved by making the transformation

$$\begin{pmatrix} \delta x \\ \delta y \end{pmatrix} = \begin{pmatrix} \cos\omega' t\sin\omega' t \\ -\sin\omega' t\cos\omega' t \end{pmatrix}\begin{pmatrix} \delta x' \\ \delta y' \end{pmatrix} \tag{11}$$

where

$$\omega' = \Omega_e\langle\sin\phi\rangle$$

In the primed coordinate system the equations are

$$\delta\ddot{x}' + \zeta\omega_s\delta\dot{x}' + \omega_s^2\delta x' + 2\zeta\omega_s\omega'\delta\dot{y}' = \cos(\omega t + \alpha)\cos\omega' t \tag{12}$$

and

$$\delta\ddot{y}' + 2\zeta\omega_s\delta\dot{y}' + \omega_s^2\delta y' - 2\zeta\omega_s\omega'\delta\dot{x}' = \cos(\omega t + \alpha)\sin\omega' t \tag{13}$$

The last term on the left-hand side of these equations can be dropped because $2\zeta\omega' \ll \omega_s$. Thus, the problem is reduced to that of solving two uncoupled differential equations, each of which describes a damped oscillator subject to periodic driving forces. Using standard Laplace transform techniques,[8] these equations can be solved to find $\delta x'$ and $\delta y'$ as functions of the flight time, input frequency, damping factor, and average latitude. Then by means of Eqs. (8) and (11) the frequency-response functions are expressed in terms of $\delta x'$ and $\delta y'$:

$$G^2(\omega,t) = \overline{(\delta x')^2}\cos^2\omega' t + \overline{2\delta x'\delta y'}\cos\omega' t\sin\omega' t + \overline{(\delta y')^2}\sin^2\omega' t \tag{14}$$

and

$$g^2(\omega,t) = \overline{(\delta y')^2}\cos^2\omega' t - \overline{2\delta x'\delta y'}\cos\omega' t\sin\omega' t + \overline{(\delta x')^2}\sin^2\omega' t \tag{15}$$

The expressions for $\delta x'$ and $\delta y'$, although straightforward to derive, are rather long and therefore not reproduced here. Plots of the response functions vs frequency are shown in Fig. 1 ($t = 5$ h) and Fig. 2 ($t = 8$ h) for a velocity error damping factor of zero and an average latitude of 60 deg. The response is very sharply peaked at the Schuler frequency, implying that the only gravity disturbance errors that will result in signifi-

cant INS errors are those with frequencies in a narrow band around this resonance frequency. Furthermore, the transverse response increases with time relative to the direct response and, after 8 h, $g^2(\omega,t)$ is larger than $G^2(\omega,t)$.

In Fig. 3, the response functions are plotted vs frequency at $t=8$ h for a velocity error damping factor $\zeta=0.1$. The damping factor has two important effects: it lowers the magnitude of both response functions dramatically and decreases the Coriolis coupling because the Coriolis term is proportional to velocity errors. Thus, damping an INS decreases the transverse response $g^2(\omega,t)$ relative to the direct response $G^2(\omega,t)$.

IV. Power Spectra of Gravity Disturbances

The calculation of the along- and cross-track disturbance error psds is greatly simplified by approximating the surface of the Earth as an infinite plane. In this flat-Earth approximation, the gravitational disturbance potential and its Fourier transform can be expressed as

$$T(x,y,z)=\int_{-\infty}^{\infty}\int_{-\infty}^{\infty}\tilde{T}(k_x,k_y,z)\exp[i(k_x x + k_y y)/R]\,dk_x dk_y \tag{16}$$

and

$$\tilde{T}(k_x,k_y,z)=\frac{1}{4\pi^2}\int_{-\infty}^{\infty}\int_{-\infty}^{\infty}T(x,y,z)\exp[-i(k_x x + k_y y)/R]\,dx dy \tag{17}$$

The variables k_x and k_y are dimensionless wave number components given by $2\pi R/\lambda_x$ and $2\pi R/\lambda_y$, respectively, where λ_x and λ_y are the wavelengths in the x and y directions and R is the mean Earth radius. The requirement that the gravitational potential above the topographic surface must satisfy Laplace's equation leads to

$$\tilde{T}(k_x,k_y,z)=\tilde{T}(k_x,k_y)e^{-kz/R} \tag{18}$$

where $\tilde{T}(k_x,k_y)$ is written in place of $\tilde{T}(k_x,k_y,0)$ for brevity and the wave number k is given by

$$k=\sqrt{k_x^2+k_y^2} \tag{19}$$

The components of the gravity disturbance vector and their Fourier transforms are related to the disturbance potential by

$$\delta g_z=\frac{\partial T}{\partial z}:\quad \delta\tilde{g}_z=-\frac{k}{R}e^{-kz/R}\tilde{T}(k_x,k_y) \tag{20}$$

$$\delta g_x=\frac{\partial T}{\partial x}:\quad \delta\tilde{g}_x=\frac{ik_x}{R}e^{-kz/R}\tilde{T}(k_x,k_y) \tag{21}$$

$$\delta g_y=\frac{\partial T}{\partial y}:\quad \delta\tilde{g}_y=\frac{ik_y}{R}e^{-kz/R}\tilde{T}(k_x,k_y) \tag{22}$$

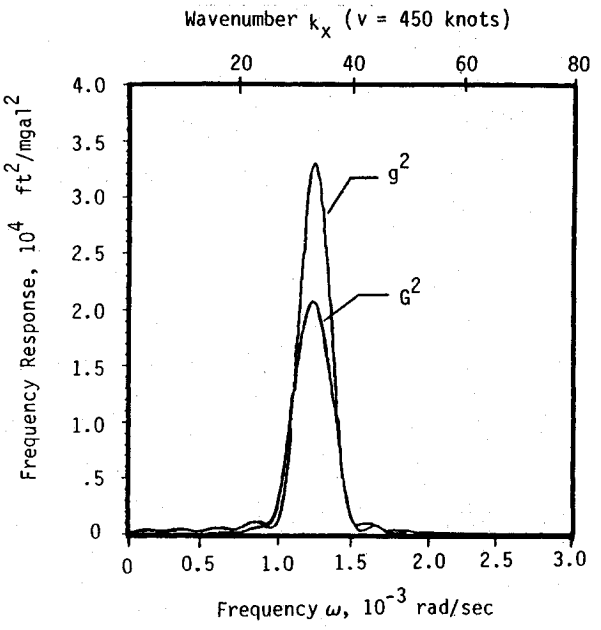

Fig. 2 Undamped response functions after 8 h.

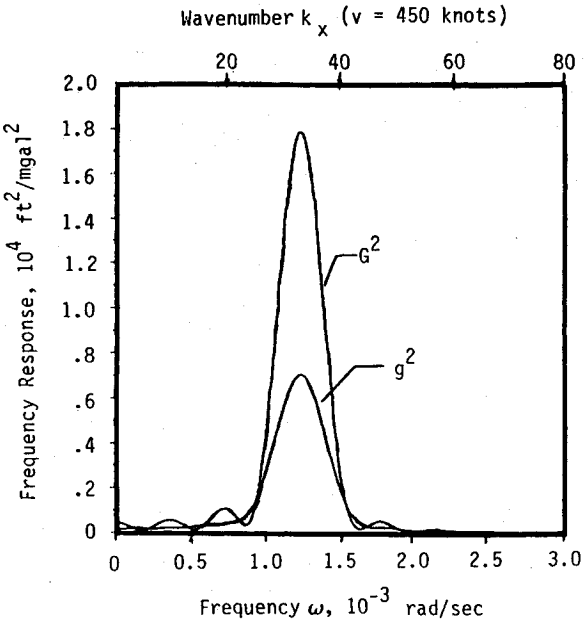

Fig. 1 Undamped response functions after 5 h.

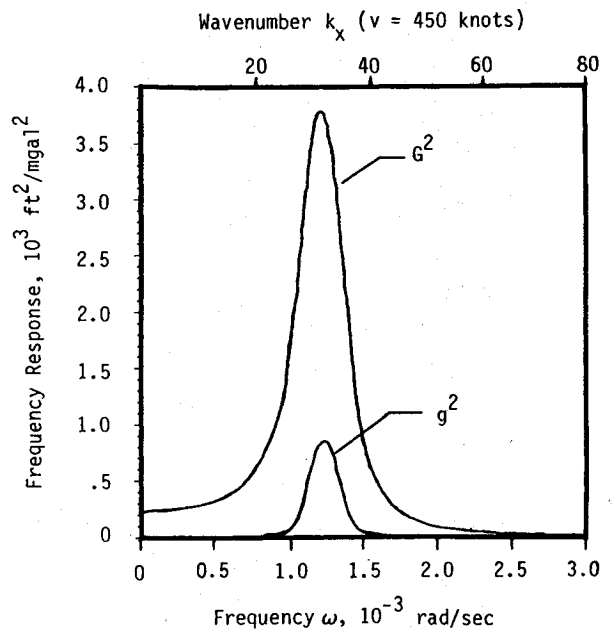

Fig. 3 Damped response functions after 8 h ($\zeta=0.1$).

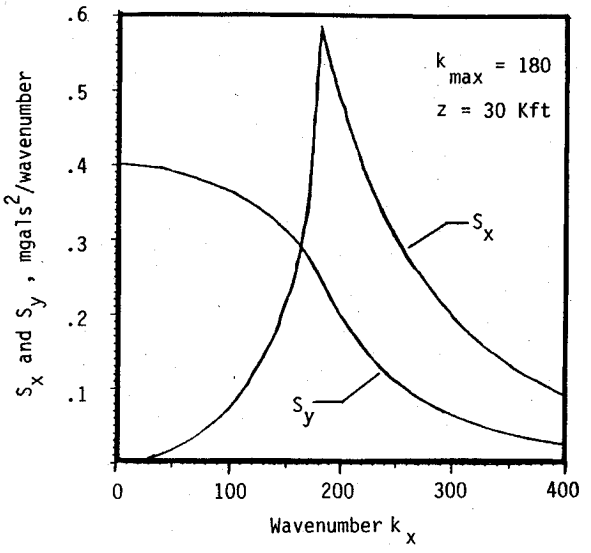

Fig. 4 Along-track (S_x) and cross-track (S_y) omission error spectra.

Equations (20-22) lead to the following relations between the horizontal gravity disturbance psds at altitude and the vertical disturbance psd at the surface:

$$S_x(k_x,k_y,z) = (k_x^2/k^2)e^{-2kz/R}S_z(k) \tag{23}$$

and

$$S_y(k_x,k_y,z) = (k_y^2/k^2)e^{-2kz/R}S_z(k) \tag{24}$$

Note that the vertical disturbance psd at the surface, $S_z(k)$, is expressed as a function of only the wave number k. This result follows immediately if the statistical properties of the vertical gravity disturbance field are isotropic. However, given that the Earth's gravitational field contains large anisotropic features in many regions, it is more reasonable to interpret $S_z(k)$ as an azimuth-averaged function rather than a function describing a fictitious isotropic field. Therefore, the resulting INS errors computed in Sec. V shall be interpreted as averages over all possible points of departure and flight azimuths.

If the aircraft moves along the x axis with speed v, then the angular frequency of gravity variations acting on the INS is given by

$$\omega = k_x v/R \tag{25}$$

All components of S_x and S_y with a given k_x contribute to a signal of frequency ω regardless of the value of k_y. Thus, the total variance of horizontal gravity disturbance errors with frequency $k_x v/R$ is calculated by integrating over all values of k_y, i.e.,

$$S_x(k_x,z) = \int_0^\infty S_x(k_x,k_y,z)\,dk_y \tag{26}$$

and

$$S_y(k_x,z) = \int_0^\infty S_y(k_x,k_y,z)\,dk_y \tag{27}$$

Using Eqs. (23-27), the one-dimensional along- and cross-track psds needed to compute the INS errors are easily obtained from the two-dimensional psd of the vertical disturbance.

It is assumed that the NGM reprsents only those gravity variations with wavelengths longer than some $\lambda_{min} = 2\pi R/k_{max}$. If, for example, the NGM is based on mean gravity disturbance values over surface elements of angular size $\theta \times \theta$, a well known rule of thumb states that $k_{max} = \pi/\theta$.[9] This relationship is consistent with the Nyquist sampling theorem, which asserts that the shortest wavelength resolved is twice the data spacing, i.e., $\lambda_{min} = 2R\theta$. Expressions for the psds of those errors due to neglecting short wavelength gravity variations for which $k > k_{max}$ (omission errors) and the errors due to incorrrectly representing the Earth's gravity field in the spectral region $k \le k_{max}$ (commission errors) are presented below. In the following, it is assumed that the NGM provides an unaliased representation of that portion of the gravity field spectrum with wave numbers less than k_{max}.

Omission Errors

According to a model proposed by Tscherning and Rapp,[7] if the vertical gravity disturbance is expanded in a series of spherical harmonics, then the term of degree n will contribute an amount C_n to the total variance where

$$C_n = \frac{A(n+1)^2 S^{n+2}}{(n-1)(n-2)(n+24)} \tag{28}$$

This expression will be used with the parameter values proposed by Schwarz,[10]

$$A = 607.57 \text{ mgal}^2 \text{ and } S = 0.998444$$

This model is relatively simple and gives an adequate representation of the degree variances over the range of degrees ($180 < n < 1000$) which most significantly affect the INS errors presented in Sec. V. Other degree variance models have been developed (see, for example, Refs. 11 and 12), and the selection of a particular model should be based upon the specific requirements for the application of interest.

The gravity variance of spherical harmonic degree n is now equated to the variance with wave number $k = n$ in the flat-Earth Fourier representation with, however, the difference that k is continuous while n assumes only integer values. The variance of degree n is mapped uniformly into a ring of radius k and width $\delta k = 1$ in the positive quadrant of the k_x-k_y plane, leading to a vertical disturbance omission error psd of

$$\begin{aligned} S_z(k) &= 2C_k/\pi k, & k > k_{max} \\ &= 0, & k \le k_{max} \end{aligned} \tag{29}$$

This equation was first derived by Bernstein.[13] More recently, Forsberg[14] has shown that the transformation from spherical harmonic degree to wave numbers in a flat-Earth Fourier representation is given more exactly by $k = n + \frac{1}{2}$. However, for the computations presented here, the simpler Bernstein transformation is used and the resulting errors are shown to be negligible.

The above expression for $S_z(k)$ is substituted into Eqs. (23) and (24), and the along- and cross-track psds are then computed using Eqs. (26) and (27). The results of such computations for $z = 30$ kilofeet (kft) and $k_{max} = 180$ (corresponding approximately to an NGM based on 1×1 deg mean gravity disturbances) are shown in Fig. 4.

The differences between the along- and cross-track spectra are quite striking. As expected, considering that wave numbers less than k_{max} have been represented in the NGM, the along-track omission error psd peaks at k_{max} and diminishes rapidly at lower values of k_x. Surprisingly, however, the cross-track psd has its maximum at $k_x = 0$, remains relatively flat out to k_{max}, and then decreases rapidly for $k_x > k_{max}$. This difference is extremely significant because at a typical aircraft speed of 450 knots the Schuler frequency correpsonds to $k_x \approx 34$, and the resonance is so sharp that the INS response is very small outside a narrow range about this value. In this range the gravity disturbance error variance in the cross-track direction is about 50 times larger than the variance in the along-track direction.

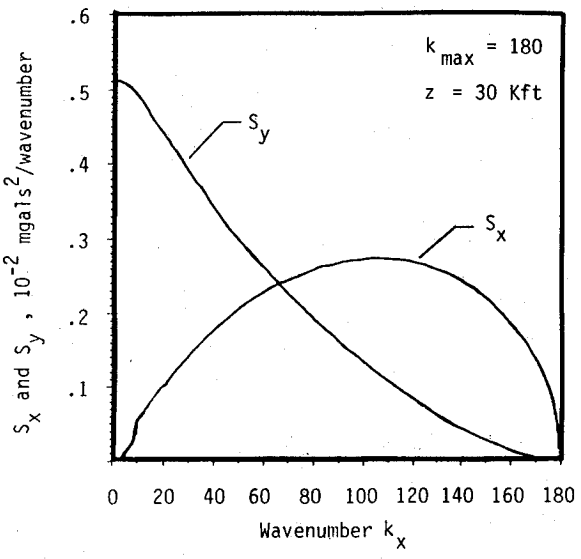

Fig. 5 Along-track (S_x) and cross-track (S_y) omission error spectra.

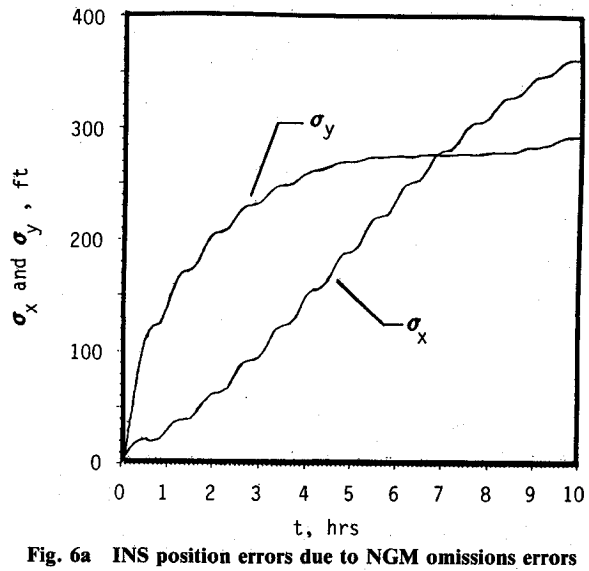

Fig. 6a INS position errors due to NGM omissions errors

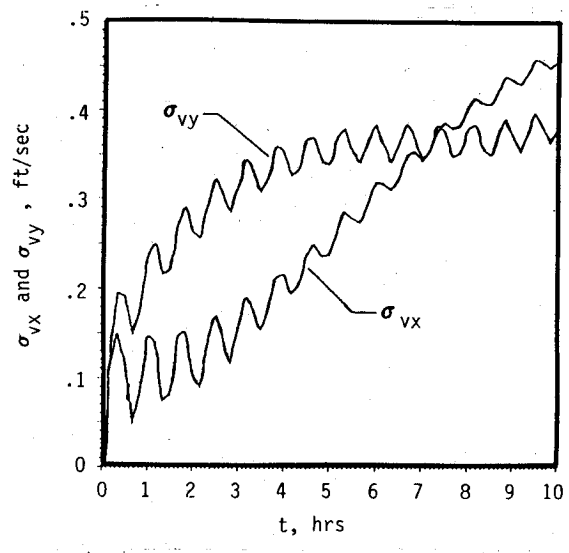

Fig. 6b INS velocity errors due to NGM omission errors.

These psd characteristics can be understood by considering certain geometrical properties of the omitted terms in the gravity disturbance potential and the resultant along- and cross-track gravity disturbance errors. The disturbance potential can be expressed in terms of an infinitude of sinusoidally varying surfaces resembling corrugated roofs, each with a particular wavelength and azimuthal direction. The along- and cross-track gravity disturbance components are the slopes of the potential function in the along- and cross-track directions, respectively. For typical aircraft speeds and sufficiently detailed gravity models, the omitted potential terms have wavelengths much shorter than the distance traveled by the aircraft during a Schuler period. Thus, for the INS to experience any disturbance near the Schuler frequency, the aircraft must be flying nearly parallel to the wave crests of an omitted term in the disturbance potential and the horizontal gravity disturbance, being perpendicular to these crests, will be nearly cross-track.

Mathematically, the short wavelength of the omission errors implies that a Fourier component capable of exciting the Schuler resonance must have $k_x \ll k$ and, therefore, from Eq. (19), $k_y \approx k$. Hence, from Eqs. (23) and (24),

$$S_x(k_x,k_y) \ll S_z(k) \quad \text{and} \quad S_y(k_x,k_y) \approx S_z(k) \tag{30}$$

when

$$k_x = \omega_s R/v$$

Thus, nearly all of the power at the Schuler frequency is in the cross-track spectrum.

Commission Errors

The vertical disturbance error psd in the spectral region $k < k_{max}$ arises from errors in the mean gravity values upon which the NGM is based. If the errors in mean gravity values in adjacent surface elements are uncorrelated, then the gravity commission error psd is well approximated as a band-limited white noise spectrum, i.e.,

$$S_z(k) = 4\sigma_g^2/\pi k_{max}^2, \quad \text{for } k \le k_{max}$$
$$= 0, \quad \text{for } k > k_{max} \tag{31}$$

where σ_g^2 is the variance of the uncorrelated mean gravity value errors. Equation (31) is used in conjuction with Eqs. (23-27) to calculate the along- and cross-track commission error psds.

The results are shown in Fig. 5 for an altitude of 30 kft and an error of 1 mgal in 1×1 deg mean gravity values (i.e., $\sigma_g = 1$ mgal when $k_{max} = 180$). These psds have some important features in common with the omission error spectra: the cross-track psd is a maximum at zero frequency and monotonically decreases as k_x increases, whereas the along-track disturbance error psd is zero at zero frequency and peaks at a value of k_x well beyond the Schuler resonance ($\omega_s R/v \approx 34$). However, these differences between the psds are much less dramatic than for omission errors. The ratio of along- to cross-track disturbance error variance at the Schuler frequency is about 2.4 for the commission error psds in Fig. 5, compared with 50 for the omission error psds.

Validation of Flat-Earth Approximation

It has been assumed that a term of degree n in a spherical harmonic expansion of the gravity potential is equivalent to a term with wave number $k = n$ in a Fourier series representation and that spherical distances along a great circle flight path are equivalent to planar distances along the x axis. It is possible to compute the omission errors psds without making these assumptions. Tscherning and Rapp[7] provided a computer program COVA, which calculates the covariances of many quantities derived from the potential, including along- and cross-track disturbances, as a function of great circle distance. An

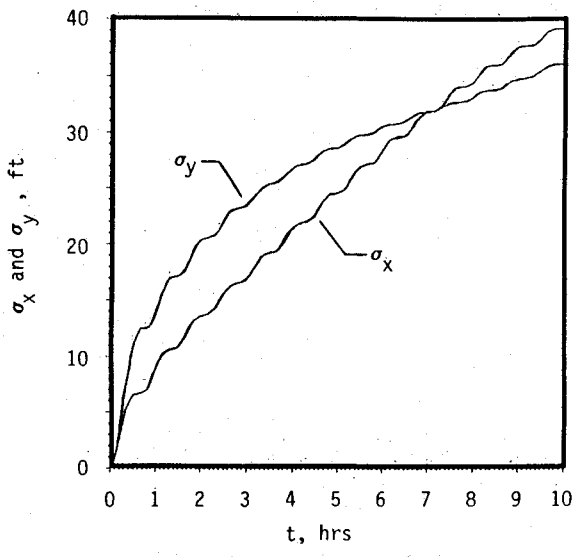

Fig. 7a INS position errors due to NGM commission errors.

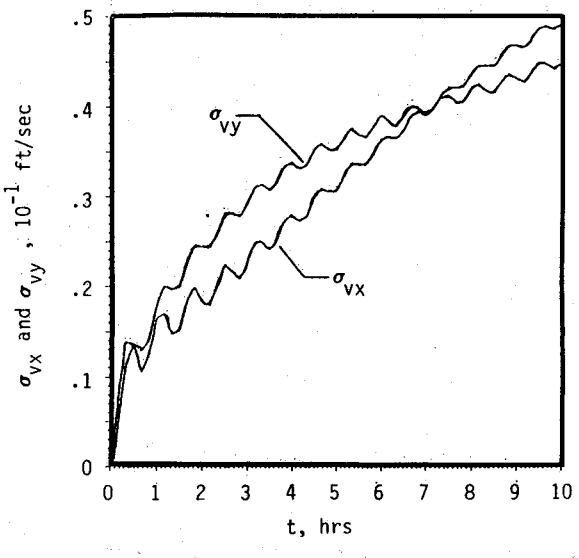

Fig. 7b INS velocity errors due to NGM commission errors.

option allows low-degree terms up to a specified degree, k_{max}, to be omitted. Thus the omission error psds can be calculated exactly, since they are the cosine transforms of these covariance functions.

This computation was carried out to obtain the along- and cross-track omission error psds for $k_{max}=20$. These psds have been compared to those calculated by means of the flat-Earth method; the agreement is remarkably good, The cross-track psds agree to within 1% over the entire frequency range. For along-track disturbances, the flat-Earth psd is 6% too large at very low wave numbers ($k_x \approx 10$), but this error decreases rapidly to less than 1% for $k_x > 40$. It is concluded that the errors resulting from the use of the flat-Earth approximation are negligible.

V. INS Errors

With expressions for both the horizontal gravity disturbance error psds and the frequency-response functions having been derived, Eqs. (3-6) can now be used to calculate the INS errors. Figures 6-9 show the position and velocity errors vs flight time for NGM errors of omission and commission. Figures 6 and 7 show the errors for an undamped INS, and Figs. 8 and 9 give the results for an INS with a velocity error damping factor of $\zeta=0.1$. In each case, the values of the other parameters are $k_{max}=180$, $z=30$ kft, $v=450$ knots, $\langle\sin\phi\rangle=0.866$, and $\sigma_g=1$ mgal.

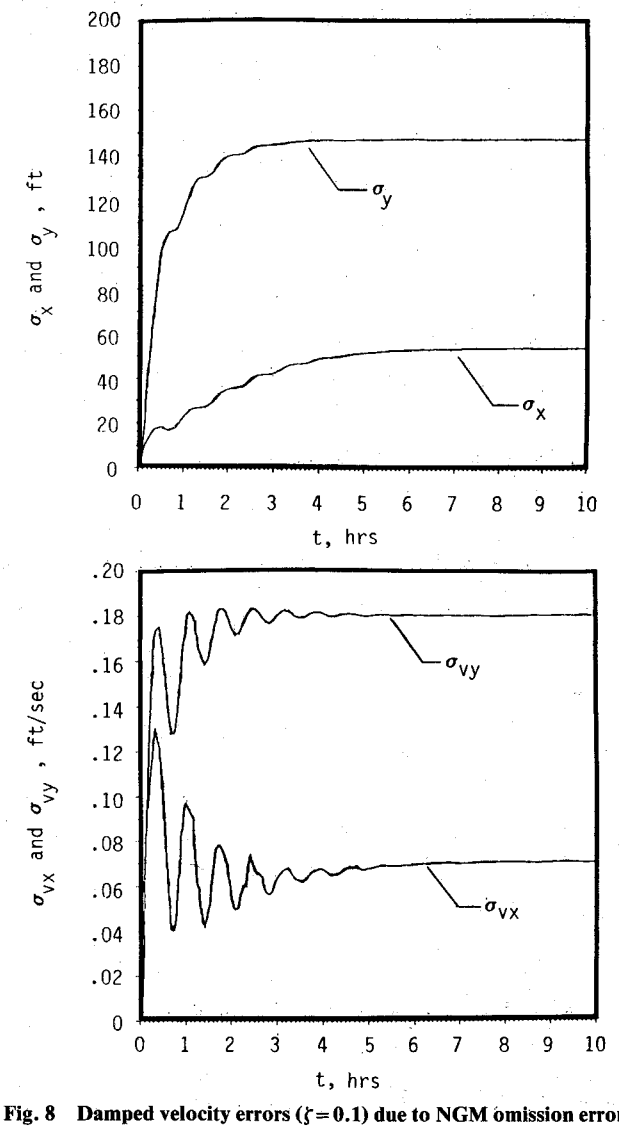

Fig. 8 Damped velocity errors ($\zeta=0.1$) due to NGM omission errors.

The undamped INS errors shown in Figs. 6 and 7 have some interesting features. There is a very noticeable difference in the rate at which along- and cross-track errors accumulate; the cross-track errors σ_y and σ_{vy} increase very quickly in the beginning of the flight and then level off, whereas the along-track errors σ_x and σ_{vx} build up more slowly at first and then increase rapidly after a few hours. This is especially true for the INS errors due to NGM omission errors. The explanation of this behavior is simple; the majority of the along-track error is due to Coriolis coupling because nearly all of the gravity error input at the Schuler frequency is in the cross-track direction. However, the Coriolis coupling does not have a large effect until the Earth has rotated through a significant portion of its 24-h cycle. As the Earth rotates, part of the cross-track error is transferred in the along-track direction. For an undamped INS, it can be shown that the time at which the errors in the two directions are equal is given approximately by

$$t_c = \frac{6}{\langle\sin\phi\rangle} \text{ hours} \tag{32}$$

Figures 8 and 9 show the errors for a damped INS ($\zeta=0.1$). There is a striking contast between these plots and those of Figs. 6 and 7. When the INS is damped, the effect of Coriolis coupling is greatly reduced; the errors reach a steady state after a few hours and the along-track error never becomes as large as the cross-track error. The steady-state magnitude of the damped INS errors is approximately equal to the

magnitude of the undamped errors after one Schuler period (84 min).

The INS errors due to NGM commission errors have been calculated assuming a 1-mgal error in the value of mean gravity over 1×1 deg surface elements. This is a reasonable value of σ_g in areas where there are about 100 well-distributed gravity measurements per 1×1-deg area (in the continental U.S. there are more measurements than this, but in most areas of the world there are considerably less). If the two-dimensional psd of gravity commission errors at the Earth's surface is band-limited white noise, as is assumed in this analysis, then the INS errors are proportional to σ_g and therefore the results given in Figs. 6-9 can be interpreted as the position or velocity errors per mgal rms error in 1×1 deg mean surface gravity values.

In Fig. 10, the position CEP (circular error probable) is plotted vs the degree of truncation, k_{max}, for INS errors due to NGM errors of omission and commission. To a good approximation, the CEP is related to the errors σ_x and σ_y by the equation $CEP = 0.589\ (\sigma_x + \sigma_y)$. The CEP due to NGM commission errors has been computed as a function of k_{max} using the result that σ_g is inversely proportional to the square root of the number of gravity measurements per surface element, which follows from the assumption that the errors in mean gravity values are uncorrelated. Because the number of measurements per surface element is proportional to the area of the element, and this area is inversely proportional to k_{max}^2, it follows that σ_g is proportional to k_{max}. Equation (31) then implies that the psd of vertical gravity disturbance commission errors remains constant as k_{max} is varied. This will be true as long as there are enough gravity measurements per surface element to ensure that correlations between errors in mean gravity values can be neglected.

It can be seen from Fig. 10 that the NGM omission errors are the dominant source of INS errors for values of k_{max} up to about 360 (corresponding to an NGM with mean gravity values on 30×30 ft surface elements). However, for detailed gravity models in which $k_{max} > 600$, the INS errors due to NGM commission errors are greater. The curves of Fig. 10 imply that, for an undamped INS on an 8-h flight path, a CEP of 75 ft is the best that can be done with the assumed density of gravity measurements. To improve on this it is necessary to decrease σ_g by increasing the survey density.

In Figs. 11 and 12, the position CEP due to NGM omission errors is plotted as a function of aircraft altitude and speed (again for an undamped INS and an 8-h flight time). Note that the CEP decreases fairly rapidly with altitude when $k_{max} = 180$; for larger values of k_{max} the attenuation of INS errors with altitude is even stronger. Figure 12 shows that for $v \geq 300$ knots the position CEP is approximately inversely proportional to the square root of the aircraft speed.

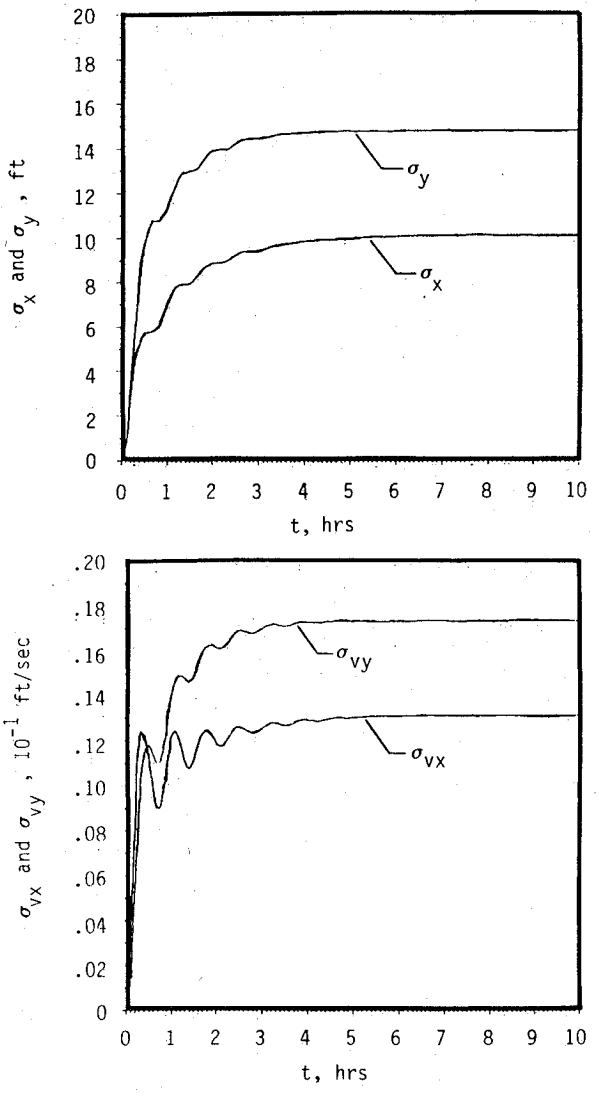

Fig. 9 Damped position errors ($\zeta = 0.1$) due to NGM commission errors.

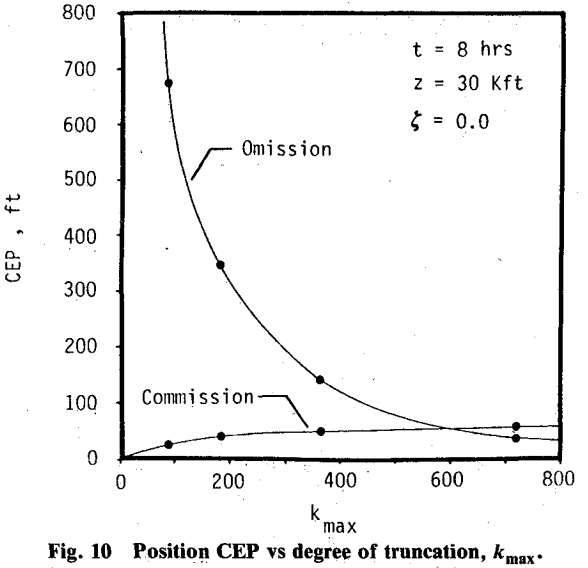

Fig. 10 Position CEP vs degree of truncation, k_{max}.

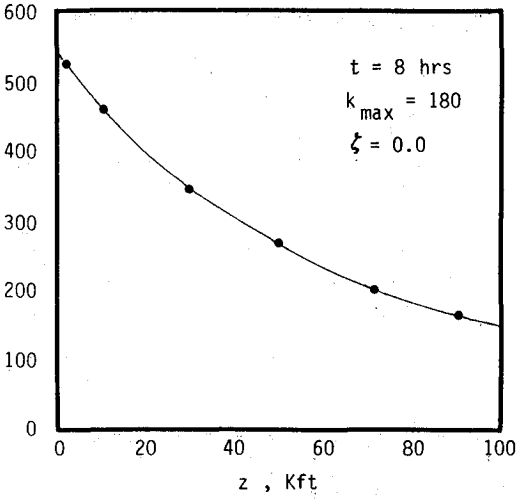

Fig. 11 Position CEP due to NGM omission errors vs altitude.

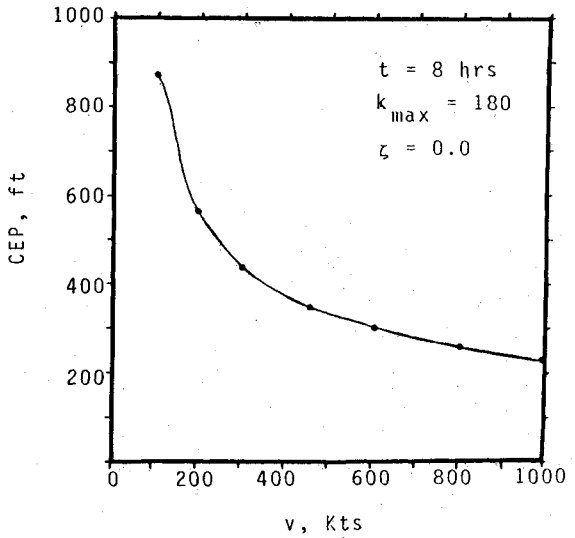

Fig. 12 Position CEP due to NGM omission errors vs aircraft speed.

VI. Limitations

The error analysis presented here has several limitations which are summarized below.

1) Although this analysis can be generalized to flight paths over which the aircraft's speed is varied, it is not easily adapted to flight paths which deviate from a great circle plane.

2) For north-south flights at low latitudes, replacing $\sin\phi$ in Eqs. (1) and (2) with its average value over the flight path is not a good approximation. However, even in these cases the predicted CEP will be nearly correct; only the separation into along- and cross-track errors is significantly affected by the Coriolis coupling term.

3) There are several sources of error in determining mean gravity values,[15] and, in general, the errors due to each of these sources are correlated to some extent. Future work should include a more realistic treatment of NGM commission errors.

4) The results given in this paper represent average INS errors over a global ensemble of flight paths. Since gravity disturbance spectra in mountainous regions differ markedly from those in topographically smooth areas, use of regional psds may be more appropriate in some applications.

VII. Conclusions

The method described herein provides an economical way of estimating the variation of gravity-induced navigation errors with the accuracy and spatial resolution of the navigation gravity model and with the flight and inertial navigation system parameters. For a given density of gravity measurements, errors arising from using gravity models with low spatial resolution are dominated by errors of omission; these are reduced as the resolution is increased until commission errors predominate. Very little is gained by increasing the resolution of the gravity model beyond this point and greater accuracy can be obtained only by densifying the gravity survey. For a survey density of about 100 gravity stations per 1×1 deg surface element, this crossover is at approximately 18 n.mi. resolution, for which the CEP is about 75 ft after 8 h of flying at 30 kft with an undamped inertial navigation system.

The power spectra of the along- and cross-track components of gravity disturbance error are very different with the result that aircraft position and velocity errors are initially induced almost exclusively in the cross-track direction. This difference in the power spectra has the additional significance that along-track disturbance errors in detailed gravity models are not well represented by the simple two-parameter Markov models that have been commonly employed in error analyses of simple ellipsoidal navigation gravity models.[16] More general Markov models with at least three parameters could be used, but care must be taken in determining the parameters because the important characteristic to model correctly is the power density at the Schuler frequency and not the variance and correlation distance as is often assumed.

The position and velocity errors resulting from gravity disturbance errors decrease significantly if the altitude or speed of the aircraft is increased. The relative magnitude of the along- and cross-track errors depends strongly on the average latitude over the flight path because this parameter determines the strength of the coupling between the channels. The velocity error damping factor reduces both the magnitude of the navigation errors and the effect of the Coriolis coupling so that the errors in a damped inertial navigation system are predominantly cross-track at all times.

References

[1]Heller, W.G. and Jordan, S.K., "Attenuated White Noise Statistical Gravity Model," *Journal of Geophysical Research,* Vol. 84, Aug. 1979, pp. 4680-4688.

[2]Shaw, L., Paul, I., and Henrikson, P., "Statistical Models for the Vertical Deflection from Gravity Anomaly Models," *Journal of Geophysical Research,* Vol. 74, Aug. 1969, pp. 4259-4265.

[3]Jordan, S.K., "Self-Consistent Statistical Models for the Gravity Anomaly, Vertical Deflection and Undulation of the Geoid," *Journal of Geophysical Research,* Vol. 77, July 1972, pp. 3660-3670.

[4]Bernstein, U. and Hess, R.I., "The Effects of Vertical Deflections on Aircraft Inertial Navigation Systems," *AIAA Journal,* Vol. 14, Oct. 1976, pp. 1377-1381.

[5]Chatfield, A.B., Bennett, M.M., and Chen, T., "Effect of Gravity Model Inaccuracy on Navigation Performance," *AIAA Journal,* Vol. 13, Nov. 1975, pp. 1494-1501.

[6]Harriman, D. and Harrison, J., "A Statistical Analysis of Gravity-Induced Errors in an Airborne INS," AIAA Paper 84-1877, Aug. 1984.

[7]Tscherning, C.D. and Rapp, R.H., "Closed Covariance Expressions for Gravity Anomalies, Geoid Undulations, and Deflections of the Vertical Implied by Anomaly Degree Variance Models," Department of Geodetic Science, Ohio State University, Columbus, OH, Rept. AFGL-TR-74-0231, May 1974.

[8]Kaplan, W., *Operational Methods for Linear Systems,* Addison-Wesley, Cambridge, MA, 1962.

[9]Rapp, R.H., "The Relationship Between Mean Anomaly Block Sizes and Spherical Harmonic Representations," *Journal of Geophysical Research,* Vol. 82, Nov. 1977, pp. 5360-5364.

[10]Shwarz, K.P., "Gravity Induced Position Errors in Airborne Inertial Navigation," Department of Geodetic Science, Ohio State University, Columbus, OH, Rept. AFGL-TR-82-0030, Dec. 1981.

[11]Moritz, H., "On the Computation of a Global Covariance Model," Department of Geodetic Science, Ohio State University, Columbus, OH, AFGL-TR-77-0163, 1977.

[12]Rapp, R.H., "Potential Coefficient and Anomaly Degree Variance Modelling Revisited," Department of Geodetic Science, Ohio State Univeristy, Columbus, OH, Rept. 293, Sept. 1979.

[13]Bernstein, U., "High Degree Geopotential Coefficient Behavior from Total Gravity Statistics," *Journal of Geophysical Research,* Vol. 80, July 1975, pp. 2947-2948.

[14]Forsberg, R., "Local Covariance Functions and Density Distributions," Department of Geodetic Science, Ohio State University, Columbus, OH, Rept. 356, June 1984.

[15]Ford, C.T., "Gravitational Model Effects on ICBM Accuracy," AIAA Paper 83-2296, Aug. 1983.

[16]Jordan, S.K., "Effects of Geodetic Uncertainties on a Damped Inertial Navigation System," *IEEE Transactions on Aerospace and Electronic Systems,* Vol. AES-9, Sept. 1973, pp. 741-752.